J. Coat. Technol. Res., **16** (5) 1411–1422, 2019
https://doi.org/10.1007/s11998-019-00223-4

A promising ternary nanohybrid of Copper@Zinc oxide intercalated with polyaniline for simultaneous antistatic and antibacterial applications

Abdolreza Mirmohseni, Maryam Azizi, Mir Saeed Seyed Dorraji

Abstract In this study, a facile and cost-effective approach has been developed for fabricating antibacterial and antistatic waterborne polyurethane (WPU)-based coatings by using Polyaniline-Copper@Zinc oxide (P-Cu@ZnO) ternary nanohybrid as a multifunctional additive. The solid-state reaction of copper acetate and zinc acetate salts led to the synthesis of copper clusters on the ZnO nanoparticles (Cu@ZnO). The obtained Cu@ZnO nanoparticles were intercalated with polyaniline (PANI) chains to prepare the P-Cu@ZnO nanohybrid. FTIR, XRD, UV–Vis, and FESEM analyses were used to characterize the structural, crystallographic, and morphological properties of the synthesized nanohybrid. Adding P-Cu@ZnO nanohybrid to the WPU matrix not only improved adhesion strength of the coatings but also enhanced their scratch resistance compared to the pristine WPU coating. Moreover, incorporation of the obtained nanohybrid into the WPU coatings caused electrical surface resistance of the obtained coatings to reach $1.2 \times 10^{+8}$ Ω/sq, so, these coatings gained the optimum electrical surface resistance to be counted as an antistatic coating. Also, the results of the colony counting test showed that the modified coatings could reduce the *Staphylococcus aureus* and *Escherichia coli* bacteria growth by about 86% and 74%, respectively.

A. Mirmohseni (✉), M. Azizi
Coating Technology Research Laboratory, Department of Applied Chemistry, Faculty of Chemistry, University of Tabriz, Tabriz, Iran
e-mail: Mirmohseni@tabrizu.ac.ir

M. S. Seyed Dorraji
Applied Chemistry Research Laboratory, Department of Chemistry, Faculty of Science, University of Zanjan, Zanjan, Iran

Keywords Ternary nanohybrid, Polyaniline-Copper@Zinc oxide, Waterborne polyurethane, Antistatic coating, Antibacterial coating

Introduction

The presence of electrostatic charge on non-conductive surfaces causes dust accumulation or even irreparable damages like explosions, etc.[1,2] Thus, to reduce these losses, creating an antistatic property in polymer coatings has become a high priority for both academic and industrial societies. In the last few years, antistatic coatings, with electrical surface resistance in the range 10^{+5}–10^{+12} Ω/sq, play an important role in industrial applications such as electrostatic paints,[3] polarization filters,[4] antistatic protection,[5] etc. A coating with both antibacterial and antistatic properties is indispensable in some special cases such as clean rooms, recovery rooms, and packing industry to guarantee the safety of people and devices.[6] Utilization of mineral nanoparticles and conducting polymers is a promising and effective way to produce antibacterial and antistatic surface coatings.[7–10]

Zinc oxide (ZnO), as one of the most used inorganic semi-conductive materials, has had an undeniable role in different fields especially antibacterial coatings.[11,12] The antibacterial mechanism of ZnO is still under debate, but the rough and abrasive surface texture of ZnO and the existence of active oxygen species on the surface of ZnO nanoparticles are the main proposed mechanisms for their antibacterial action.[13,14] ZnO nanoparticles can be combined with other materials which lead to the improved properties and synergistic effect of the constituents.[15,16] The compositions of ZnO and copper, with the excellent antibacterial characteristics in comparison with each component, could be counted as a candidate for the production of antibacterial products.[17,18]

Polyaniline (PANI) as the most prevalent conducting polymer has many advantages such as low production cost, the facile method of synthesis, and high environmental stability.[19,20] Therefore, it has commonly been used in rechargeable batteries, sensors, anti-corrosion coatings, and antistatic materials.[19,21–23] Utilization of pure PANI to create favorable conduction property in the coatings requires increased content of conducting polymer in the formulation that would lead to the poor mechanical stability of the final product.[24,25] Some studies suggest that performance of pure PANI can be improved by blending with some inorganic nanoparticles such as silica, titanium dioxide, etc.[26–28] In this regard, the combination of pure PANI with metal and metal oxide nanoparticles like Cu and ZnO leads to the production of a nanohybrid with outstanding properties due to synergic interfacial molecular interactions between the three components.[29–32]

In this study, we combined distinct properties of three components: ZnO, metallic Cu, and pure PANI to utilize resulting synergistic features for improving the waterborne polyurethane (WPU) based coatings' properties. For this purpose, first, the nanostructured Cu@ZnO was produced and then was intercalated with PANI to obtain the multifunctional nanohybrid. This nanohybrid was incorporated into the waterborne polyurethane dispersion (WPUs) to prepare antistatic and antibacterial coating without deterioration of WPU coating's original properties. Crystallographic, structural, and morphological characteristics of the prepared nanohybrid were investigated by XRD, FTIR, UV–Vis, and FESEM analyses. The final coatings were also studied in terms of mechanical, antistatic, and antibacterial properties.

Experimental

Materials

Hydrochloric acid (HCl, 37%), aniline monomer, ammonium persulfate (APS), copper(II) acetate monohydrate (98%), and zinc acetate dihydrate (99%) were purchased from Sigma–Aldrich Company. Polycaprolactone (MW = 2000 g/mol) was obtained from Shenzhen Esun Industrial Co., Ltd. Isophorone diisocyanate (IPDI, 98%), 2,2-Bis(hydroxymethyl)propionic acid (DMPA, 98%), dibutyltin dilaurate (DBTDL, 95%), ethylenediamine (EDA, 99%), and triethylamine (TEA, 99.5%) were purchased from Merck Company.

Preparation of copper decorated zinc oxide (Cu@ZnO)

Cu@ZnO nanoparticles were synthesized by a facile solid-state reaction. In this procedure, zinc acetate dihydrate (0.0027 mol) and copper acetate monohydrate (0.0025 mol) were thoroughly mixed by using a pestle and mortar, and then transferred to a silica crucible. The silica crucible was placed in a muffle furnace, and thermal process was initiated by setting the final temperature to 300°C (increasing at the rate of 4°C/min). After reaching 300°C, the reaction was continued at 300°C for 3 h to turn the color of the mixture from bluish-green to dark-brown. Finally, the crucible was cooled and the synthesized nanoparticles were collected (Fig. 1).

Synthesis of pure polyaniline (PANI) and Polyaniline-Copper@Zinc oxide ternary nanohybrid (P-Cu@ZnO)

The conventional oxidative polymerization method was used to prepare pure PANI. First, 0.028 mol of aniline monomer was dispersed in HCl (1 M) and was stirred for 1 h. Then, APS (0.025 mol) was dissolved in HCl (1 M) and was added dropwise to the above mixture. The temperature of the mixture was fixed at 0°C, and the reaction was allowed to continue at this temperature for 6 h. Finally, the dark-green precipitates were collected by filtration and dried at 60°C.

In order to prepare the ternary nanohybrid, the same procedure was followed with the difference that Cu@ZnO nanoparticles (0.14 g) were dispersed in aniline monomer's mixture prior to the addition of APS (Fig. 2).

Preparation of waterborne polyurethane dispersion (WPUs)

Waterborne polyurethane dispersion was prepared in a four-necked flask equipped with a condenser, dropping funnel, mechanical stirrer, and thermometer. 17.70 g of Polycaprolactone, 1.86 g of DMPA, and 0.02 g of DBTDL were charged in the flask and the temperature was kept at 80°C until the polycaprolactone melted. Then, 10.57 g of IPDI was added to the flask and the reaction was continued at the same temperature until the NCO number (isocyanate functional groups) reached a specified value (6.25%). The NCO number was detected by di-*n*-butylamine back titration method.[33] The obtained prepolymer was neutralized by the addition of 0.92 g of TEA. Then, the reaction's temperature was decreased to 25°C and DI water (70 g) was added dropwise with vigorous agitation. Immediately after the addition of water, 1.46 g of EDA was added to the reactor and, finally, WPU dispersion with 33 wt% solids content was obtained.

Fig. 1: Preparation of Cu@ZnO nanoparticles

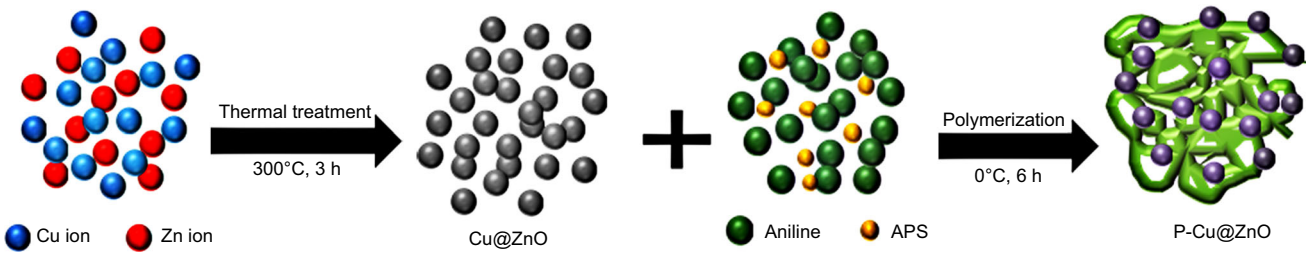

Fig. 2: Schematic illustration of the preparation of P-Cu@ZnO ternary nanohybrid

Preparation of modified waterborne polyurethane coatings

In order to obtain antistatic and antibacterial WPU-based coatings, the various contents of pure PANI, Cu@ZnO, and P-Cu@ZnO were added to the WPU dispersions. The modified dispersions were cast on Teflon and steel substrates and dried for 4 h at 50°C. The prepared coatings were labeled as pristine WPU, WPU-PANI, WPU-Cu@ZnO, and WPU-P-Cu@ZnO, respectively.

Characterization

Instruments

Fourier transform infrared spectra of the samples were obtained using Perkin-Elmer spectrometer (USA) in the range 400–4000 cm^{-1}. X-ray diffraction (XRD) patterns were taken by using Bruker D8 ADVANCE X-ray Diffractometer (USA), in the 2θ ranging from 4° to 70°. UV–Visible spectra of the samples were obtained by using UV/Vis–1800, Shimadzu Spectrophotometer (Japan). Nanotrac Wave apparatus (Microtrac Company, USA) was utilized for recording dynamic light scattering (DLS) diagram. The surface morphology of the obtained products was investigated using Tescan—Mira III Scanning Electron Microscope (Czech Republic).

Pull-off adhesion test

The adhesion strength of the WPU-based coatings on steel substrates was evaluated by a pull-off adhesion tester (ERICHSEN, model: 525, Germany) based on the ASTM D 4541. For this purpose, aluminum dollies were glued on the surface of the WPU coatings by utilizing a strong two-part adhesive. All coatings were kept at ambient temperature for 24 h to make sure the glue fully cured. Finally, the coated surrounding area of each dolly was scraped, and then, the dolly was pulled off by a gradually increasing pull-off force until the WPU coating detached from the steel substrate. The required force for detachment of the coating was recorded as the adhesion strength of the coating. All tests were performed three times to ensure the repeatability of measurements.

Evaluating scratch resistance

The hardness and scratch resistance of the WPU-based coatings were determined according to the ISO 1518 standard using a Pen Hardness Tester (model TQC, Netherlands). In this method, a pen-like device with a tungsten carbide tip is dragged on the coating's surface. The amount of applied force to the coating is determined by the three springs with adjustable hardness. The hardness of the coating or its scratch resistance is determined by the force of hardest spring that causes damage on the surface of the coating specimen.

Investigation of antistatic behavior

According to ASTM D257, the two-point probe technique was used to measure the electrical surface resistance of the pristine and modified WPU coatings. A constant electrical potential (1000 V) was applied to the free-standing films (10 × 10 × 0.3 cm) by a digital insulation tester (MASTECH MS5203), and the electrical resistance of the coatings (R_R) was recorded. The antistatic behavior of the coatings was evaluated by the electrical surface resistance (R_s) that is calculated by equation (1):

$$R_s = \frac{p}{g} \times R_R \quad (1)$$

where R_s is the calculated electrical surface resistance (Ω/sq), R_R is the recorded electrical resistance (Ω), P is the utilized probes' parameter (cm), and g is the distance between inner electrodes (cm).

Antibacterial studies

The antibacterial activity of the WPU coatings modified by the ternary nanohybrid and each of its components (i.e., pure PANI and Cu@ZnO) was evaluated by the colony counting method. For this purpose, both gram-positive and gram-negative bacterial strains were investigated and the bacterial species: *Staphylococcus aureus* (*S. aureus*) and *Escherichia coli* (*E. coli*) were chosen as models. In this method, sterile blank paper disks coated with 20 μL of the modified WPU dispersion were put in contact with a certain volume of bacterial suspension with determined concentration. After 60 min, 100 μL of the above suspension was spread on the plates containing solidified agar, and then, the plates were incubated at 37°C for 24 h. The visual and quantitative assessments of the reduction of bacterial colonies were used as a criterion for the samples' antibacterial activity. All tests were repeated three times.

Results and discussion

Characterization of Polyaniline-Copper@Zinc oxide ternary nanohybrid

Structural and crystallographic analyses

Fourier transform infrared spectra of pure PANI, Cu@ZnO, and P-Cu@ZnO are shown in Fig. 3a. In the FTIR spectrum of pure PANI, the bands at 1555 and 1485 cm^{-1} are assigned to the –C=C stretching mode of quinoid and benzenoid rings in the structure of PANI, respectively. The bands at 1285–1299 cm^{-1} correspond to C–N stretching vibration of the secondary aromatic amine.[30] The C–H bending vibrations of the aromatic rings are observed at 785 and 1099 cm^{-1}.[34] As shown in the FTIR spectrum of Cu@ZnO nanoparticle, the characteristic absorption bonds of Zn–O and hydroxyl groups, which exist on the ZnO nanoparticles, appear at 533 and 3398 cm^{-1}, respectively. Two bands at 624 and 835 cm^{-1} are assigned to Cu–O bond[35] which may exist on the Cu@ZnO nanoparticles. All the peaks of two components (PANI and Cu@ZnO) can be observed in the FTIR spectrum of P-Cu@ZnO nanohybrid. Also, these absorption peaks experience some dislocations which originate from weak interactions between PANI and Cu@ZnO nanoparticle.

X-ray diffraction patterns of pure PANI, Cu@ZnO, and P-Cu@ZnO are illustrated in Fig. 4b. The low and broad peaks appeared at 2θ = 19.1° and 23.9° (interlayer spacing = 4.68 and 3.77 Å) indicate the amorphous state of PANI.[34] In the XRD pattern of the Cu@ZnO nanoparticle, the clear and strong peaks at 2θ = 31.82°, 34.49°, 36.32°, 56.50°, and 62.92° (100, 002, 101, 110, and 103 planes reflection) are ascribed to ZnO, and the presence of two characteristic peaks diffracted at 2θ = 43.20° and 50.44° (from 111 and 200 planes) is a confirmation for the formation of copper clusters.[36] Furthermore, the characteristic peak at 2θ = 42.20 is attributed to CuO which may be produced as an impurity in the synthesis process of Cu@ZnO nanoparticles. In the XRD spectrum of the P-Cu@ZnO sample, all the peaks of both components (i.e., PANI and Cu@ZnO) can be observed and the small displacements are attributed to weak interactions between the two components.

Confirmation of the presence of Cu clusters in Cu@ZnO nanoparticles by UV–Vis study

Some nanoparticles of transition metals show surface plasmon resonance band in UV–Vis spectra,[37–39] and metallic copper (Cu) nanoparticles also have a plasmon resonance peak in the wavelength range from 500 to 600 nm.[40] Tracking this peak can be an efficient method for determining the metallic state of the elements in different compositions. The UV–Vis spectra of pure PANI and ternary nanohybrid are presented in Fig. 4. As exhibited in Fig. 4a, two peaks at 290 and 430 nm are related to π–π^* transitions of pure PANI.[31] In the P-Cu@ZnO spectrum, the appearance of the plasmon resonance band at 580 nm confirms the presence of copper clusters in P-Cu@ZnO nanohybrid, besides, PANI peaks can also be observed in this spectrum (Fig. 4b). These results are in agreement with the results of XRD spectroscopy.

Morphological study

Figure 5 exhibits FESEM images of pure PANI, Cu@ZnO nanoparticles, and P-Cu@ZnO nanohybrid. As shown in Figs. 5a and 5b, pure PANI is composed

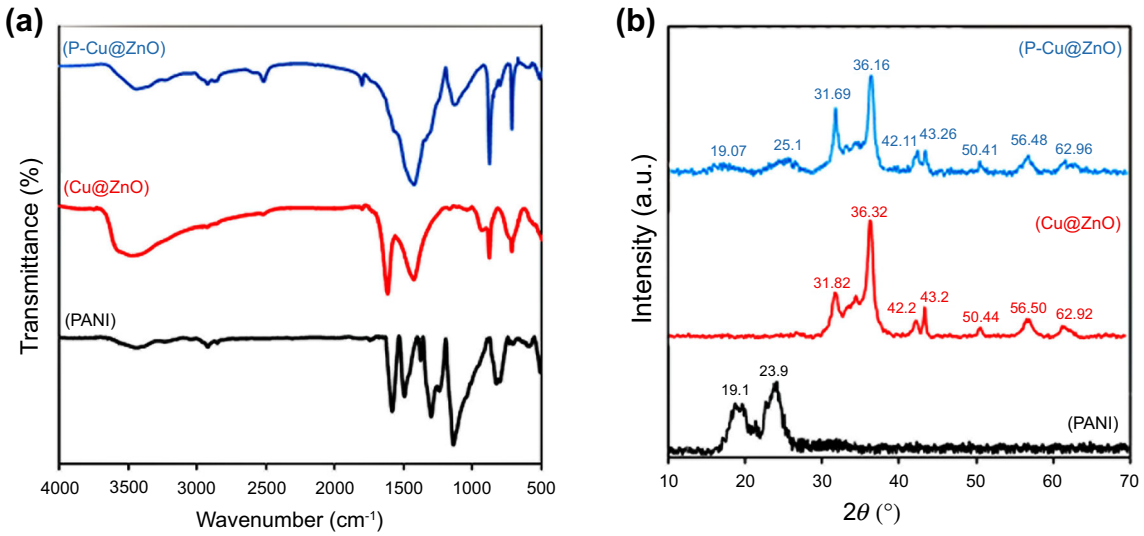

Fig. 3: FTIR spectra (a) and XRD patterns (b) of pure PANI, Cu@ZnO, and P-Cu@ZnO

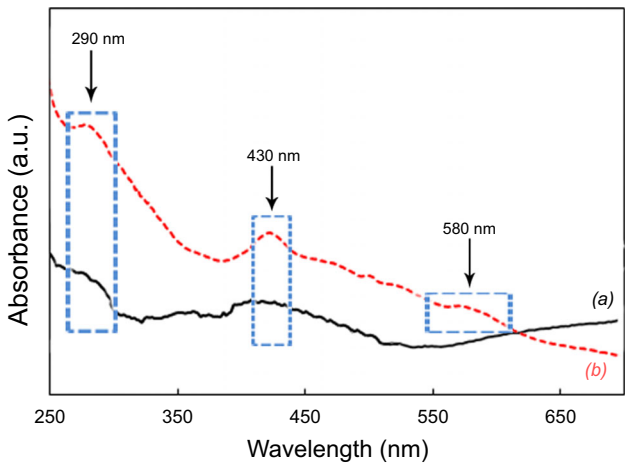

Fig. 4: UV–Vis spectra of pure PANI (a) and P-Cu@ZnO ternary nanohybrid (b)

of irregularly shaped agglomerates and granular particulates. The Cu@ZnO nanoparticles have a spherical structure (Figs. 5c and 5d) due to the control of the reaction time and temperature during thermal treatment (3 h and 300°C). The FESEM image of Cu@ZnO shows that the amount of oxidized copper was negligible because if metallic copper converted into CuO, copper's morphology would change to a rod-like structure,[36] while such a structure could not be observed in Figs. 5c and 5d.

The intercalation between Cu@ZnO nanoparticles and PANI chains is fairly evident in the FESEM images of P-Cu@ZnO nanohybrid (Figs. 5e and 5f). The placement of Cu@ZnO nanoparticles among PANI chains prevents their aggregation and leads to the increased interactions between the components, so that enhances their synergistic effects on each other. Therefore, FESEM images of P-Cu@ZnO nanohybrids can prove the improved properties of ternary nanohybrid compared to its constituents.

The proposed mechanism for the formation of copper clusters on the zinc oxide

In the literature, several mechanisms have been reported for the synthesis of various compounds of copper and zinc oxide that each of them could contain different forms of copper and zinc oxide.[17,41] In this work, according to the FESEM images which clearly show Cu clusters on the ZnO nanoparticles and also based on Krishnamurthi et al. research,[36] a unique mechanism can be proposed for preparing Cu@ZnO nanoparticles. As shown in Fig. 6, water is fully eliminated at 300°C (step 1). Then, in the presence of oxygen and zinc acetate, copper acetate can be converted into metallic copper (Cu), and carbon dioxide gas (CO_2) is also liberated (step 2). In the third step, zinc oxide nanoparticles are produced through the two different reactions (step 3). If the reaction continues longer than the prescribed time (3 h), because of the presence of excess O_2 in the system, the rate of the reaction's final step (step 4) is accelerated and all the metallic copper converts into copper oxide.[36] All steps of this proposed mechanism are confirmed by the various analyses which were mentioned earlier.

Evaluation of the coatings' adhesion strength and scratch resistance

The results of adhesion strength and scratch resistance of the WPU-based coatings on steel substrates are presented in Table 1 and Fig. 7a. As illustrated in Table 1, the pull-off adhesion strength of the pristine

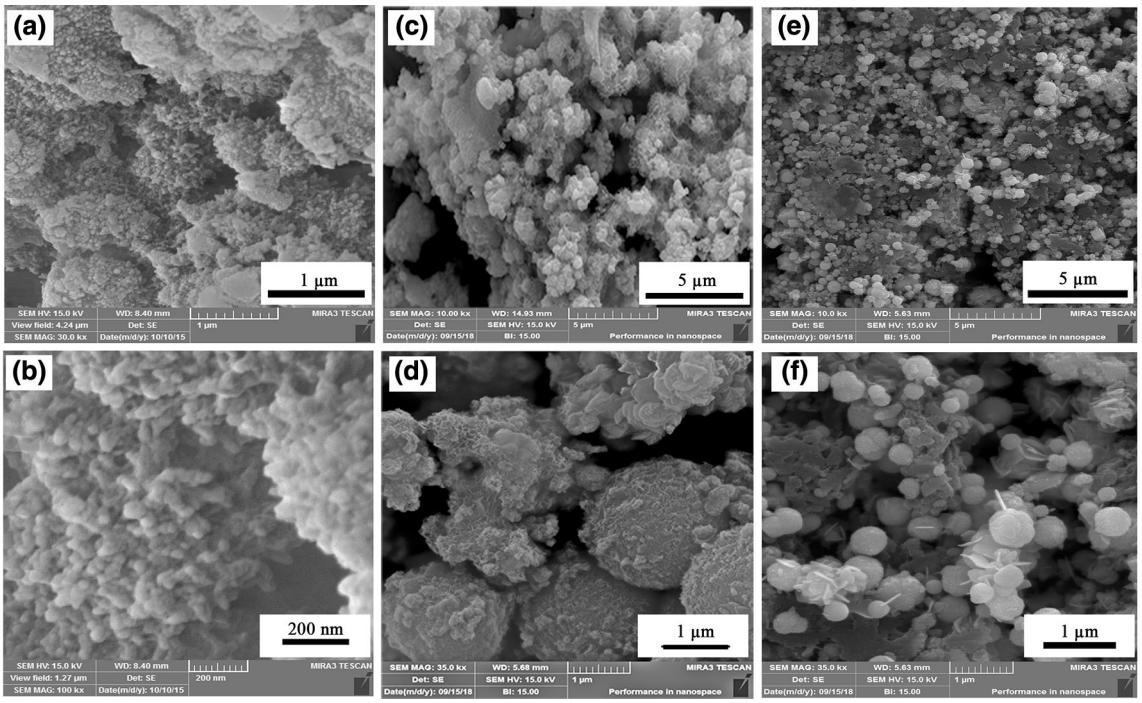

Fig. 5: FESEM images of pure PANI (a, b), Cu@ZnO nanoparticles (c, d), and P-Cu@ZnO nanohybrid (e, f)

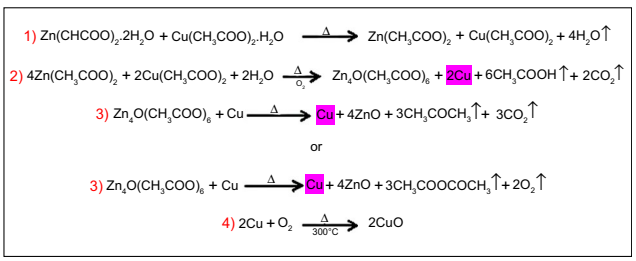

Fig. 6: The proposed mechanism for the formation of copper clusters (Cu) on zinc oxide (ZnO)[36]

WPU coating, without any additive, is equal to 7.1 MPa. This remarkable adhesion strength of the pristine WPU coating is mainly attributed to some functional groups of the WPU chains and particle size distribution of the pristine WPU dispersion. The existence of some functional groups like N–H and C=O on WPU chains, which is confirmed by appearance of the peaks at 3332 and 1722 cm^{-1} in the FTIR spectrum of WPU dispersion (Fig. 7b),[42] endow WPU coating with the ability to strongly adhere to the steel substrate. Also, the fine size of WPU dispersion's particles (10–70 nm, Fig. 7c) is another reason for the high adhesion strength of the pristine WPU coating that was obtained by casting of the WPU dispersion.[43] In the case of WPU coatings modified by 5 wt% pure PANI, Cu@ZnO, and P-Cu@ZnO, the adhesion strength values are equal to 7.2, 7.4, and 7.7 MPa, respectively. The improved adhesion strengths in the WPU-PANI and WPU-Cu@ZnO coatings (Table 1) could be attributed to charged and porous surface of PANI and the presence of ZnO and metallic Cu, which all enhance the hydrophilicity of the modified coatings. Eventually, the hydrophilic and polar nature of the obtained coatings boosts the adhesion of polyurethane coating to the polar surface of the mild steel.[44] Therefore, the coating which benefits from the simultaneous presence of PANI and Cu@ZnO (WPU-P-Cu@ZnO, 5 wt%) could have more adhesion strength than the coatings modified by separate pure PANI and Cu@ZnO, individually.

The complete detachment of the coating from the steel substrate is referred to as the adhesion failure, while the cohesion failure means the partial detachment of the coating (Fig. 7d). As illustrated in Table 1, both adhesion and cohesion failures happened in different samples after the pull-off tests. The complete form of adhesion failure is observed in the pristine WPU, while WPU-PANI, WPU-Cu@ZnO, and WPU-P-Cu@ZnO show the different extents of the cohesion failure. These observations can be explained by a competition which occurs between adhesion bonds of matrix–substrate and cohesion bonds of matrix–matrix.

The scratch resistance of the WPU coatings was measured by the pen hardness test, and the obtained results are summarized in Table 1. The received values of this test show that the scratch resistance of the pristine WPU coating is equal to 5.00 N, while the modified WPU coatings resist against scratching forces which are equal to 5.10–5.50 N. These results show that the existence of pure PANI, Cu@ZnO, and P-Cu@ZnO in the WPU matrix renders the modified coatings more scratch resistant compared with the pristine coating. In other words, interactions between

Table 1: Results of adhesion strength tests and scratch resistance tests of the WPU-based coatings

Samples	Adhesion strength (MPa)	Failure type (%)	Scratch resistance (N)
pristine WPU	7.10 ± 0.10	100% Adhesion	5.00 ± 0.05
WPU- PANI	7.20 ± 0.10	25% Cohesion	5.10 ± 0.05
WPU- Cu@ZnO	7.40 ± 0.10	40% Cohesion	5.35 ± 0.05
WPU- P-Cu@ZnO	7.70 ± 0.15	80% Cohesion	5.50 ± 0.05

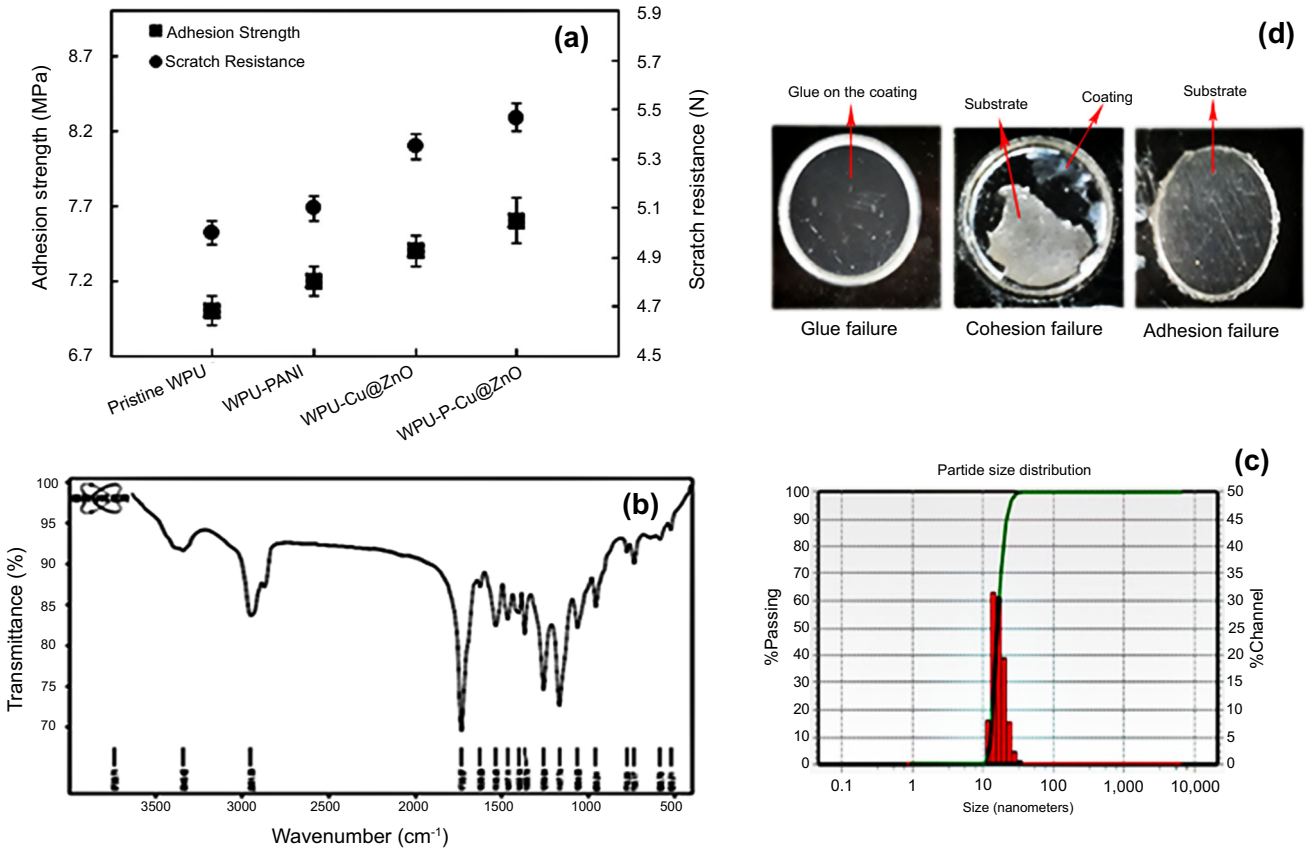

Fig. 7: The results of adhesion strength and scratch resistance tests of the WPU-based coatings (Error bars are the standard deviation, *n* = 3) (a), FTIR spectrum and DLS diagram of the WPU dispersion (b, c), and an illustration of types of the occurred failures after the pull-off test (d)

polyurethane chains and these polar additives reduce the movements of WPU chains and prevent them from tearing apart.

Antistatic behavior of waterborne polyurethane based coatings

The ability of the WPU-based coatings to dissipate electrostatic charges or their antistatic behavior was evaluated by measuring their electrical surface resistance. As shown in Fig. 8, the pristine WPU coating, without any additive, exhibits high electrical surface resistance about $1.5 \times 10^{+14}$ Ω/sq, so it is categorized as an electrically insulating coating. Addition of an appropriate amount of conductive additives to the WPU matrix to reach the percolation threshold cause the creation of three-dimensional conduction pathways throughout the polymer matrix, and the electrical surface resistance of the obtained coating begins to reduce. The presence of 3 wt% pure PANI (i.e., percolation threshold), due to benefiting from a conjugated structure, reduces the electrical surface resistance of the WPU coating to $2.5 \times 10^{+9}$ Ω/sq (Fig. 8a).[45] As shown in Fig. 8b, the electrical surface resistance of the WPU coatings reaches $4.0 \times 10^{+10}$ Ω/sq by addition of 3 wt% Cu@ZnO nanoparticles. It is obvious that utilizing pure PANI and Cu@ZnO,

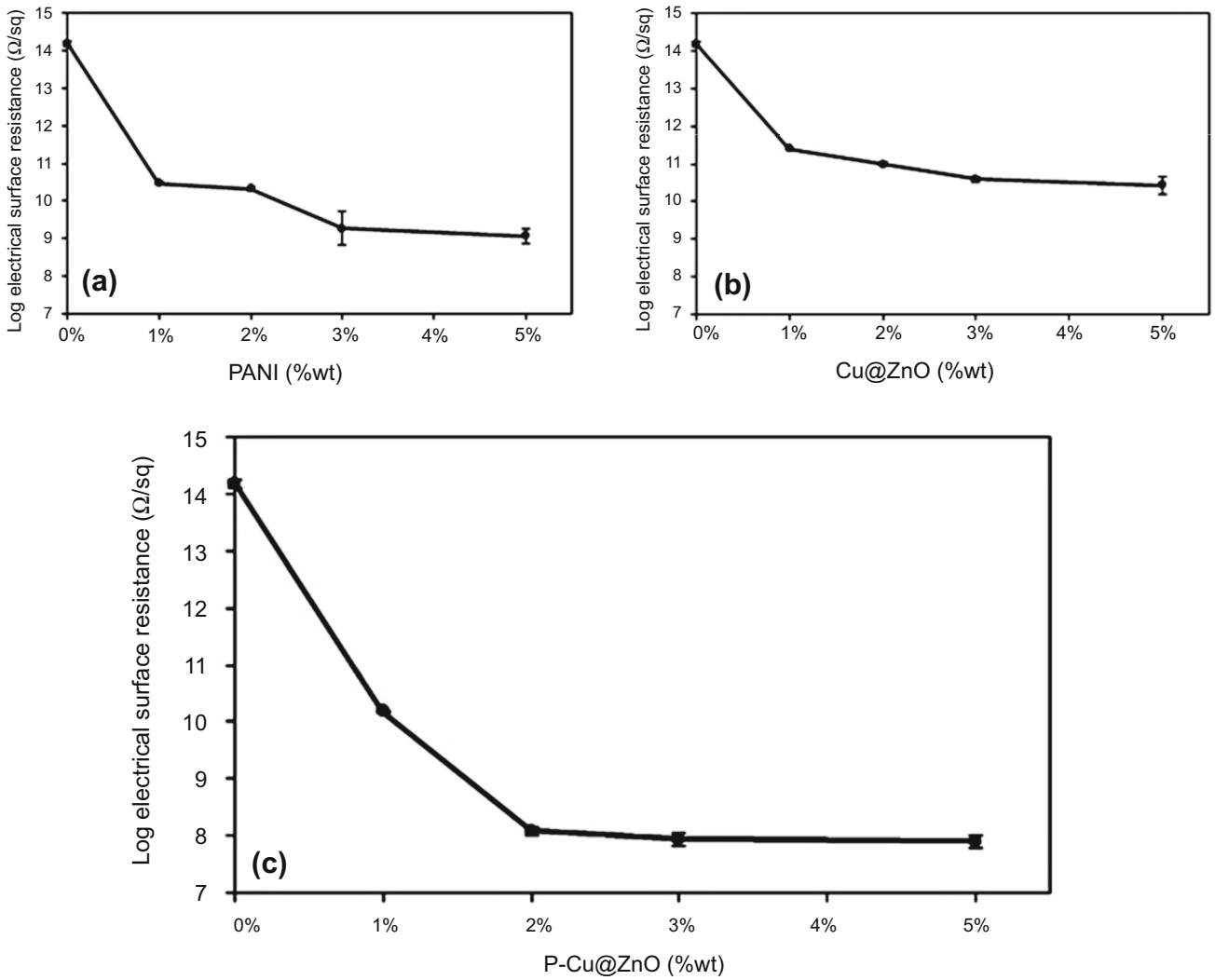

Fig. 8: Electrical surface resistance of the WPU coatings modified by PANI (a) Cu@ZnO (b), and P-Cu@ZnO nanohybrid (c). Error bars are the standard deviation (n = 3)

individually, does not induce the satisfactory antistatic property in the WPU coatings.

As shown in Fig. 8c, the P-Cu@ZnO nanohybrid is more effective in reducing the electrical surface resistance of the WPU coatings in comparison with separate PANI and Cu@ZnO. The percolation threshold of P-Cu@ZnO is equal to 2 wt% which causes the electrical surface resistance of the WPU-P-Cu@ZnO coating to decrease to $1.2 \times 10^{+8}$ Ω/sq that falls within the range of antistatic coatings' electrical surface resistance. This high ability of ternary nanohybrid to improve the antistatic properties of the WPU coatings is attributed to the effect of both constituents (i.e., PANI and Cu@ZnO). The interactions between the conjugated structure of PANI chains and highly conductive copper clusters, which exist on the Cu@ZnO nanoparticles, lead to creating the connections between PANI chains. This phenomenon not only decreases the required amount of the nanohybrid for the creation of three-dimensional conducting paths throughout the coating's matrix but also enhances its effectiveness in reducing the electrical surface resistance of the WPU-based coatings.

Investigating antibacterial activity of the waterborne polyurethane coatings

The antibacterial behavior of the pristine WPU, WPU-PANI, WPU-Cu@ZnO, and WPU- P-Cu@ZnO coatings was evaluated against two gram-positive (*Staphylococcus aureus*) and gram-negative (*Escherichia coli*) bacteria. The results of the colony counting method (Figs. 9,10) show that the pristine WPU coating does not inhibit the growth of gram-positive and gram-negative bacteria, while the addition of pure PANI (5 wt%) to the WPU coating causes the slight inhibition of *S. aureus* growth and its cell reduction is equal to 23%. This antibacterial action is attributed to the positive surface charges of doped PANI and the

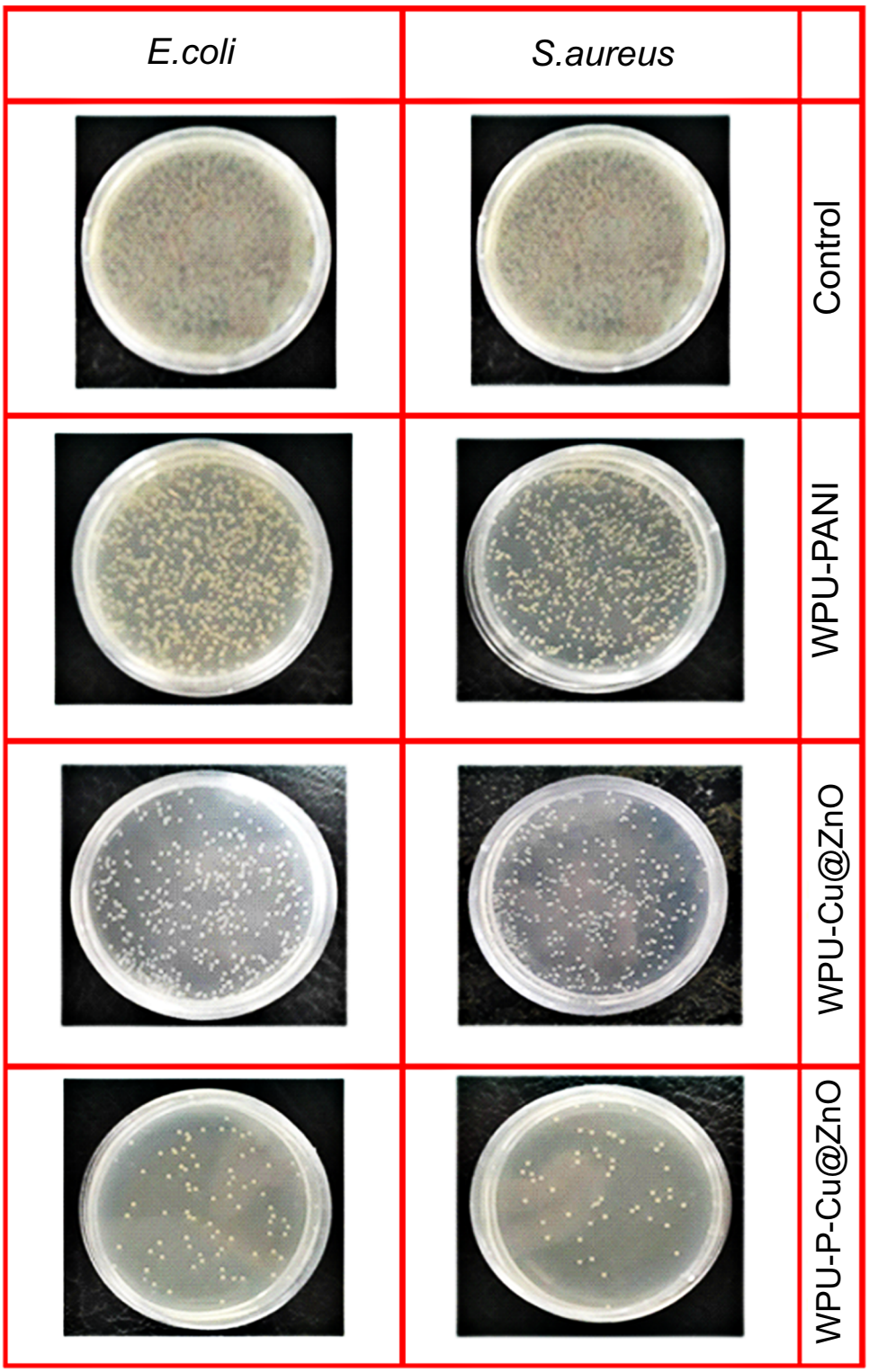

Fig. 9: Results of the antibacterial behavior of the pristine WPU coatings (Control) and the WPU coatings containing 5 wt% of pure PANI, Cu@ZnO nanoparticle, and P-Cu@ZnO nanohybrid in contact with *S. aureus* and *E. coli* bacteria

electrostatic interactions between the PANI and the negative surface of the bacteria.[46]

The presence of 5 wt% Cu@ZnO nanoparticles in the WPU coating has a significant effect on the elimination of the bacteria and leads to a reduction in growth rate of the gram-positive bacteria (64%) after 24 h. The release of copper ions from Cu@ZnO nanoparticles and their interaction with the sulfur

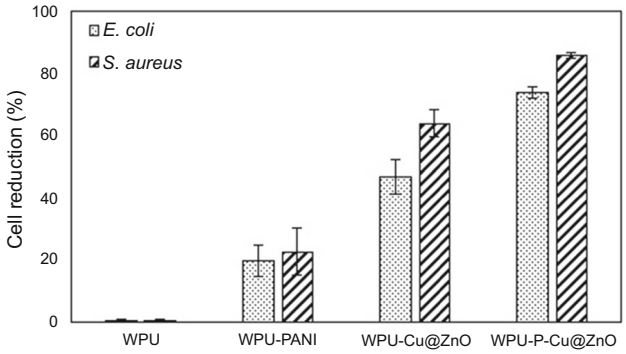

Fig. 10: Determination of cell reduction rates by the colony counting method. Error bars are the standard deviation (*n* = 3)

groups of membrane's proteins could interrupt some vital bacterial processes.[47] The synergetic effect between the two mentioned mechanisms (electrostatic interactions and copper ion release) in ternary P-Cu@ZnO nanohybrid could create a strong antibacterial property in the WPU coating modified by the ternary nanohybrid. Therefore, loss of viability of *E. coli* and *S. aureus* bacteria by the WPU-P-Cu@ZnO coating is equal to 74% and 86%, respectively.

As can be seen, the growth inhibition of gram-positive bacteria in all of the coatings is more than the gram-negative counterpart (Fig. 9). The vulnerability of gram-positive bacteria seems reasonable because the lipid bilayer of gram-negative bacteria's membrane acts as a hydrophobic barrier.[48] Therefore, the penetration of hydrophilic copper ions into the gram-negative bacteria's hydrophobic membrane is more difficult than the gram-positive ones.

Conclusion

The main importance of this study was the preparation of the multifunctional ternary nanohybrid and benefiting from its unique features to create simultaneous antistatic and antibacterial properties in the WPU-based coatings. The Cu@ZnO nanoparticles were prepared by the solid-state reaction of copper acetate and zinc acetate, and then, they were intercalated with PANI to obtain the P-Cu@ZnO ternary nanohybrid. Structural, crystallographic, and morphological properties of the synthesized PANI, Cu@ZnO, and P-Cu@ZnO were investigated by FTIR, XRD, UV–Vis, and FESEM analyses. Incorporation of P-Cu@ZnO nanohybrid into the WPU coatings significantly improved the adhesion strength and scratch resistance of the modified coatings. Besides, this ternary nanohybrid not only reduced the electrical surface resistance of the coatings to $1.2 \times 10^{+8}$ Ω/sq but also improved their inhibitory action against *E. coli* (74% cell reduction) and *S. aureus* (86% cell reduction). Therefore, the produced WPU-P-Cu@ZnO coating has a great potential to be coated on the different surfaces in operating rooms, clean rooms and anywhere else which demands WPU characteristics along with simultaneous antimicrobial and antistatic properties.

Acknowledgements The authors thank the University of Tabriz for financial and other support.

References

1. Hazle, J, Harmon, R, Dang, HT, ''Composition for Transparent Antistatic Coating.'' US Patent 9778399B2, 2017
2. Ren, J, Zheng, L, Wang, Y, Zang, X, Wu, J, Yue, Y, Wu, X, Han, L, ''Synthesis and Characterization of Quaternary Ammonium Based Ionic Liquids and Its Antistatic Applications for Diesel.'' *Colloids Surf. A Physicochem. Eng. Asp.*, **556** 239–247 (2018)
3. Yang, Q, Ma, Y, Zhu, J, Chow, K, Shi, K, ''An Update on Electrostatic Powder Coating for Pharmaceuticals.'' *Particuology*, **31** 1–7 (2017)
4. Guntermann U, Elschner, A, Kirchmeyer, S, ''Conductive Polymer Layer as an Antistatic Protection Shield for Polarization Filter.'' US Patent 20150064449A1, 2015
5. Mirmohseni, A, Azizi, M, Dorraji, MSS, ''Facile Synthesis of Copper/Reduced Single Layer Graphene Oxide as a Multifunctional Nanohybrid for Simultaneous Enhancement of Antibacterial and Antistatic Properties of Waterborne Polyurethane Coating.'' *Prog. Org. Coat.*, **131** 322–332 (2019)
6. Wang, J, Zhang, C, Du, Z, Li, H, Zou, W, ''Functionalization of MWCNTs with Silver Nanoparticles Decorated Polypyrrole and Their Application in Antistatic and Thermal Conductive Epoxy Matrix Nanocomposite.'' *RSC Adv.*, **6** (38) 31782–31789 (2016)
7. Chen, W, Liu, P, Liu, Y, Wang, Q, Duan, W, ''A Temperature-Induced Conductive Coating Via Layer-by-Layer Assembly of Functionalized Graphene Oxide and Carbon Nanotubes for a Flexible, Adjustable Response Time Flame Sensor.'' *Chem. Eng. J.*, **353** 115–125 (2018)
8. Chen, W, Liu, P, Liu, Y, Wang, Q, Duan, W, ''A Temperature-Induced Conductive Coating Via Layer-by-Layer Assembly of Functionalized Graphene Oxide and Carbon Nanotubes for a Flexible, Adjustable Response Time Flame Sensor.'' *Chem. Eng. J.*, **353** 115–125 (2018)
9. Jiang, Y, Sun, R, Zhang, H-B, Min, P, Yu, D, Yang, Z-Z, ''Graphene-Coated ZnO Tetrapod Whiskers for Thermally and Electrically Conductive Epoxy Composites.'' *Compos. Part A Appl. Sci. Manuf.*, **94** 104–112 (2017)
10. Olad, A, Rezvani, F, Nosrati, R, ''Preparation and Characterization of Polyurethane Based Self-Cleaning and Antibacterial Coating Containing Silver Ion Exchanged Montmorillonite/TiO_2 Nanocomposite.'' *Res. Chem. Intermed. J.*, **44** (3) 1711–1727 (2018)
11. Seki, Y, Seki, Y, ''Development of Conductivity of Acrylic Polymer Using Ionic Liquids Incorporated with Zinc Oxide Nanoparticles.'' *Polym. Plast. Technol. Eng.*, **56** (18) 1942–1948 (2017)
12. Kattel, S, Ramírez, PJ, Chen, JG, Rodriguez, JA, Liu, P, ''Active Sites for CO_2 Hydrogenation to Methanol on Cu/ZnO Catalysts.'' *Science*, **355** (6331) 1296–1299 (2017)

13. Padmavathy, N, Vijayaraghavan, R, ''Enhanced Bioactivity of ZnO Nanoparticles—AN Antimicrobial Study.'' *Sci. Technol. Adv. Mater.*, **9** (3) 035004 (2008)
14. Fiedot, M, Maliszewska, I, Rac-Rumijowska, O, Suchorska-Woźniak, P, Lewińska, A, Teterycz, H, ''The Relationship Between the Mechanism of Zinc Oxide Crystallization and Its Antimicrobial Properties for the Surface Modification of Surgical Meshes.'' *Materials*, **10** (4) 353 (2017)
15. Bai, X, Wang, L, Zong, R, Lv, Y, Sun, Y, Zhu, Y, ''Performance Enhancement of ZnO Photocatalyst via Synergic Effect of Surface Oxygen Defect and Graphene Hybridization.'' *Langmuir*, **29** (9) 3097–3105 (2013)
16. Fu, H, Jiang, Y, Ding, J, Zhang, J, Zhang, M, Zhu, Y, Li, H, ''Zinc Oxide Nanoparticle Incorporated Graphene Oxide as Sensing Coating for Interferometric Optical Microfiber for Ammonia Gas Detection.'' *Sens. Actuator B Chem.*, **254** 239–247 (2018)
17. Bhuyan, T, Khanuja, M, Sharma, R, Patel, S, Reddy, M, Anand, S, Varma, A, ''A Comparative Study of Pure and Copper (Cu)-Doped ZnO Nanorods for Antibacterial and Photocatalytic Applications with Their Mechanism of Action.'' *J. Nanopart. Res.*, **17** (7) 288 (2015)
18. Mirmohseni, A, Rastgar, M, Olad, A, ''Preparation of PANI–CuZnO Ternary Nanocomposite and Investigation of Its Effects on Polyurethane Coatings Antibacterial, Antistatic, and Mechanical Properties.'' *J. Nanostruct. Chem.*, **8** (4) 473–481 (2018)
19. Mirmohseni, A, Gharieh, A, Khorasani, M, ''Waterborne Acrylic–Polyaniline Nanocomposite as Antistatic Coating: Preparation and Characterization.'' *Iran. Polym. J.*, **25** (12) 991–998 (2016)
20. Zhu, A, Wang, H, Sun, S, Zhang, C, ''The Synthesis and Antistatic, Anticorrosive Properties of Polyaniline Composite Coating.'' *Prog. Org. Coat.*, **122** 270–279 (2018)
21. Jiménez, P, Levillain, E, Alévêque, O, Guyomard, D, Lestriez, B, Gaubicher, J, ''Lithium n Doped Polyaniline as a High Performance Electroactive Material for Rechargeable Batteries.'' *Angew. Chem. Int. Ed. Engl.*, **56** (6) 1553–1556 (2017)
22. Wang, J, Wang, X, Tang, H, Gao, Z, He, S, Li, J, Han, S, ''Ultrasensitive Electrochemical Detection of Tumor Cells Based on Multiple Layer CdS Quantum Dots-Functionalized Polystyrene Microspheres and Graphene Oxide–Polyaniline Composite.'' *Biosens. Bioelectron.*, **100** 1–7 (2018)
23. Caldas, CM, Calheiros, LFG, Soares, B, ''Silica/Polyaniline Hybrid Materials Prepared by Inverse Emulsion Polymerization for Epoxy/Based Anticorrosive Coating.'' *J. Appl. Polym. Sci.*, **134** (47) 45505 (2017)
24. Liu, B-T, Syu, J-R, Wang, D-H, ''Conductive Polyurethane Composites Containing Polyaniline-Coated Nano-Silica.'' *J. Colloid Interface Sci.*, **393** 138–142 (2013)
25. Chiou, WC, Han, JL, Lee, SN, ''Synthesis and Studies of the Physical Properties of Polyaniline and Polyurethane-Modified Epoxy Composites.'' *Polym. Eng. Sci.*, **48** (2) 345–354 (2008)
26. Al-Sagur, H, Komathi, S, Karakaş, H, Atilla, D, Gürek, A, Basova, T, Farmilo, N, Hassan, A, ''A Glucose Biosensor Based on Novel Lutetium Bis-Phthalocyanine Incorporated Silica-Polyaniline Conducting Nanobeads.'' *Biosens. Bioelectron.*, **102** 637–645 (2018)
27. Roy, AS, ''Antistatic and Dielectric properties of One-Dimensional Al^{2+}: Nd_2O_3 Nanowire Doped Polyaniline Nanocomposites for Electronic Application.'' *Sensor Actuat A-Phys.*, **280** 1–7 (2018)
28. Radoičić, MB, Milošević, MV, Miličević, DS, Suljovrujić, EH, Ćirić-Marjanović, GN, Radetić, MM, Šaponjić, ZV, ''Influence of TiO_2 Nanoparticles on Formation Mechanism of PANI/TiO_2 Nanocomposite Coating on PET Fabric and Its Structural and Electrical Properties.'' *Surf. Coat. Technol.*, **278** 38–47 (2015)
29. Zhybak, MT, Vagin, MY, Beni, V, Liu, X, Dempsey, E, Turner, AP, Korpan, YI, ''Direct Detection of Ammonium Ion by Means of Oxygen Electrocatalysis at a Copper-Polyaniline Composite on a Screen-Printed Electrode.'' *Microchim. Acta*, **183** (6) 1981–1987 (2016)
30. Anand, A, Rani, N, Saxena, P, Bhandari, H, Dhawan, SK, ''Development of Polyaniline/Zinc Oxide Nanocomposite Impregnated Fabric as an Electrostatic Charge Dissipative Material.'' *Polym. Int.*, **64** (9) 1096–1103 (2015)
31. Olad, A, Nosrati, R, ''Preparation, Characterization, and Photocatalytic Activity of Polyaniline/ZnO Nanocomposite.'' *Res. Chem. Intermediat. J.*, **38** (2) 323–336 (2012)
32. Darvishnejad, M, Ebrahimzadeh, H, ''Magnetic Halloysite Nanotube/Polyaniline/Copper Composite Coupled with Gas Chromatography–Mass Spectrometry: A Rapid Approach for Determination of Nitro-Phenanthrenes in Water and Soil Samples.'' *J. Chromatogr. A*, **1563** 1–9 (2018)
33. Rath, S, Chavan, J, Sasane, S, Srivastava, A, Patri, M, Samui, A, Chakraborty, B, Sawant, SN, ''Coatings of PDMS-Modified Epoxy via Urethane Linkage: Segmental Correlation Length, Phase Morphology, Thermomechanical and Surface Behavior.'' *Prog. Org. Coat.*, **65** (3) 366–374 (2009)
34. Omar, FS, Numan, A, Duraisamy, N, Ramly, MM, Ramesh, K, Ramesh, S, ''Binary Composite of Polyaniline/Copper Cobaltite for High Performance Asymmetric Supercapacitor Application.'' *Electrochim. Acta*, **227** 41–48 (2017)
35. Yu, Q, Huang, H, Chen, R, Wang, P, Yang, H, Gao, M, Peng, X, Ye, Z, ''Synthesis of CuO Nanowalnuts and Nanoribbons from Aqueous Solution and Their Catalytic and Electrochemical Properties.'' *Nanoscale*, **4** (8) 2613–2620 (2012)
36. Krishnamurthi, P, Raju, Y, Khambhaty, Y, Manoharan, PT, ''Zinc Oxide-Supported Copper Clusters with High Biocidal Efficacy for *Escherichia coli* and *Bacillus cereus*.'' *ACS Omega*, **2** (6) 2524–2535 (2017)
37. Amendola, V, Pilot, R, Frasconi, M, Marago, OM, Iati, MA, ''Surface Plasmon Resonance in Gold Nanoparticles: A Review.'' *J. Phys. Condens. Matter*, **29** (20) 203002 (2017)
38. Chen, S, Sommers, JM, ''Alkanethiolate-Protected Copper Nanoparticles: Spectroscopy, Electrochemistry, and Solid-State Morphological Evolution.'' *J. Phys. Chem. B*, **105** (37) 8816–8820 (2001)
39. Huang, YF, Zhang, M, Zhao, LB, Feng, JM, Wu, DY, Ren, B, Tian, ZQ, ''Activation of Oxygen on Gold and Silver Nanoparticles Assisted by Surface Plasmon Resonances.'' *Angew. Chem. Int. Ed. Engl.*, **53** (9) 2353–2357 (2014)
40. Zhang, P, Song, T, Wang, T, Zeng, H, ''In-situ Synthesis of Cu Nanoparticles Hybridized with Carbon Quantum Dots as a Broad Spectrum Photocatalyst for Improvement of Photocatalytic H2 Evolution.'' *Appl. Catal. B*, **206** 328–335 (2017)
41. Jin, J, Fang, LJ, Tang, L, Ji, P, Wang, C S, Wang, HP, ''Preparation of Nano Cu-ZnO/PET Fiber for Antibacterial Application.'' *Mater. Sci. Forum*, Trans Tech Publ, Year
42. Delpech, MC, Miranda, GS, ''Waterborne Polyurethanes: Influence of Chain Extender in Ftir Spectra Profiles.'' *Cent. Eur. J. Eng.*, **2** (2) 231–238 (2012)
43. Wang, N, Lu, L, Zhang, Y, ''Effect of the Particle Size in Dispersions on the Properties of Waterborne Polyurethane/Casein Composites.'' *Ind. Eng. Chem. Res.*, **43** (13) 3336–3342 (2004)

44. Wu, C-G, Chen, J-Y, ''Chemical Deposition of Ordered Conducting Polyaniline Film via Molecular Self-Assembly.'' *Chem. Mater.*, **9** (2) 399–402 (1997)
45. Chen, C-H, Kan, Y-T, Mao, C-F, Liao, W-T, Hsieh, C-D, ''Fabrication and Characterization of Water-Based Polyurethane/Polyaniline Conducting Blend Films.'' *Surf. Coat. Technol.*, **231** 71–76 (2013)
46. Kumar, R, Oves, M, Almeelbi, T, Al-Makishah, NH, Barakat, M, ''Hybrid Chitosan/Polyaniline-Polypyrrole Biomaterial for Enhanced Adsorption and Antimicrobial Activity.'' *J. Colloid Interface Sci.*, **490** 488–496 (2017)
47. Chatterjee, AK, Chakraborty, R, Basu, T, ''Mechanism of Antibacterial Activity of Copper Nanoparticles.'' *Nanotechnology*, **25** (13) 135101 (2014)
48. Nosrati, R, Olad, A, Najjari, H, ''Study of the Effect of TiO_2/Polyaniline Nanocomposite on the Self-Cleaning Property of Polyacrylic Latex Coating.'' *Surf. Coat. Technol.*, **316** 199–209 (2017)